



# Highly dispersed ceria on activated carbon for the catalyzed ozonation of organic pollutants

Alexandra Gonçalves<sup>a</sup>, Joaquín Silvestre-Albero<sup>b</sup>, Enrique V. Ramos-Fernández<sup>b</sup>,  
Juan Carlos. Serrano-Ruiz<sup>b</sup>, José J.M. Órfão<sup>a</sup>, Antonio Sepúlveda-Escribano<sup>b,\*\*</sup>,  
Manuel Fernando R. Pereira<sup>a,\*</sup>

<sup>a</sup> Laboratório de Catálise e Materiais (LCM), Laboratório Associado LSRE/LCM, Departamento de Engenharia Química, Faculdade de Engenharia, Universidade do Porto, Rua Dr. Roberto Frias, 4200-465 Porto, Portugal

<sup>b</sup> Laboratorio de Materiales Avanzados, Instituto Universitario de Materiales de Alicante - Departamento de Química Inorgánica, Universidad de Alicante, Apartado 99, E-03080 Alicante, Spain

## ARTICLE INFO

### Article history:

Received 28 September 2011

Received in revised form

26 November 2011

Accepted 29 November 2011

Available online 7 December 2011

### Keywords:

Catalytic ozonation

Cerium oxide

Activated carbon

Oxalic acid

Aniline

## ABSTRACT

Several catalysts of cerium oxide highly dispersed on activated carbon were prepared varying the cerium precursor, the solvent and the chemical surface properties of the support, and characterized by several techniques. Afterwards, these materials were investigated as ozonation catalysts for the mineralization of two organic compounds (oxalic acid and aniline). The ozonation results were compared with those obtained in the absence of catalyst and in the presence of the parent activated carbons used for the preparation of these materials. The prepared catalysts have better performances than the parent activated carbons, denoting a clear synergic effect between activated carbon and cerium oxide. The efficiency of the catalysts is mainly affected by the amount of Ce<sup>3+</sup> species on the surface. However, in the ozonation of oxalic acid, the specific surface area and metal oxide particle diameter also played an important role. The use of activated carbon as support favors the removal of both organic compounds studied. Highly dispersed cerium oxide on activated carbon shows better catalytic performance than a composite with the same composition.

© 2011 Elsevier B.V. All rights reserved.

## 1. Introduction

Catalytic ozonation is an innovative technology for the elimination of organic compounds in water and wastewater. Ozone preferentially attacks molecules containing unsaturated bonds, leading to the formation of saturated compounds such as aldehydes, ketones and carboxylic acids. Due to their low reactivity towards ozone, these compounds tend to accumulate in water. Therefore, single ozonation is not sufficient to achieve a high mineralization degree. To overcome this drawback, ozonation processes are being modified in order to increase their oxidizing capability. Some studies have shown that several metals in solution or in the solid phase under various forms (salts, oxides, supported metals) may catalyze ozonation reactions, being able to destroy more recalcitrant pollutants [1]. Activated carbon by itself has been proven to be an efficient ozonation catalyst [2–5]. In previ-

ous studies, activated carbon/cerium oxide composites were tested in the ozonation of organic compounds, and they showed better results in the mineralization of the mentioned compounds in comparison to those obtained using activated carbon or cerium oxide [6,7]. In the present manuscript we intend to develop even more active catalysts by using highly dispersed cerium oxide on activated carbon. In this way, the available surface area of the cerium oxide will increase significantly as well as the electron transfer between ceria and activated carbon. Recently, the development of highly dispersed CeO<sub>2</sub> on activated carbon [8] and the preparation of carbon nanotubes/cerium oxide composites have been reported in the literature [8,9]. Some novel synthesis techniques for highly dispersed ceria nanoparticles on carbon materials have been developed. Namely, CeO<sub>2</sub>/AC samples prepared by the impregnation method with cerium nitrate salt [8,10], CeO<sub>2</sub>/CNT core-shell nanowires prepared under boiling reflux of ethylene glycol [11], CeO<sub>2</sub>/CuO/CNT nanocomposites synthesized using CNTs as templates by a pyridinothermal method [12] and necklace-like CeO<sub>2</sub>/CNT composites prepared by a simple solvothermal method [13].

The present work aimed at the assessment of materials containing highly dispersed cerium oxide on activated carbon as catalysts for ozonation and to investigate a possible synergic effect between activated carbon and cerium oxide in the ozonation of organic

\* Corresponding author. Tel.: +351 225 081 468; fax: +351 225 081 449.

\*\* Corresponding author. Tel.: +34 965 90 3974; fax: +34 965 90 3974.

E-mail addresses: [agg@fe.up.pt](mailto:agg@fe.up.pt) (A. Gonçalves), [joaquin.silvestre@ua.es](mailto:joaquin.silvestre@ua.es)

(J. Silvestre-Albero), [E.V.RamosFernandez@tudelft.nl](mailto:E.V.RamosFernandez@tudelft.nl) (E.V. Ramos-Fernández), [jcserrano@ua.es](mailto:jcserrano@ua.es) (J. Carlos. Serrano-Ruiz), [jjmo@fe.up.pt](mailto:jjmo@fe.up.pt) (J.J.M. Órfão), [asepul@ua.es](mailto:asepul@ua.es) (A. Sepúlveda-Escribano), [fpereira@fe.up.pt](mailto:fpereira@fe.up.pt) (M.F.R. Pereira).

compounds. Several catalysts were prepared varying the cerium precursor (Ce(III) or Ce(IV)), the solvent (water or acetone), and the support (basic or acidic activated carbon), following a procedure similar to that described in Ref. [10]. The catalytic activity of the cerium oxide/activated carbon samples prepared was investigated in the ozonation of two selected compounds: oxalic acid (short chain carboxylic acid) and aniline (aromatic compound containing an amine substituent). Oxalic acid was selected because it is a common final oxidation product resulting from several organic pollutants and it is usually refractory to single ozonation [14–16]. Aniline is an aromatic amine that was found to be easily oxidized by single ozonation in a wide range of solution pHs, but its mineralization requires the use of advanced oxidation processes [17]. For comparison, experimental results obtained with the parent activated carbon samples used for the preparation of catalysts were also included.

## 2. Experimental

### 2.1. Preparation and characterization of materials

A commercial activated carbon supplied by Mead Westvaco (Nuchar RGC30), with 0.5–1.0 mm particle size, was used as initial support and labeled as “AC”. This material was treated for 24 h at room temperature with an aqueous solution of  $\text{H}_2\text{O}_2$  (17 v/v%). Then, it was washed with ultrapure water, until no oxidant character was detected using an acid aqueous solution of  $\text{KMnO}_4$ , and dried at 373 K for 12 h (sample “ACox”). Each carbon sample was impregnated with solutions of two different cerium salts, a Ce(IV) precursor ( $(\text{NH}_4)_2[\text{Ce}(\text{NO}_3)_6]$ ) and a Ce(III) precursor ( $\text{Ce}(\text{NO}_3)_3 \cdot 6\text{H}_2\text{O}$ ), with the adequate concentration to obtain a nominal  $\text{CeO}_2$  loading of 20 wt.%. Actual loadings were determined by repetitive calcinations and weighting; a value of  $20.0 \pm 0.5$  wt.% was obtained. In the preparation stage two different solvents were used, water (named as “w”) or acetone (named as “k”). The excess of solvent was removed by gentle heating and finally samples were dried at 373 K overnight. The decomposition of the cerium precursor to obtain  $\text{CeO}_2/\text{AC}$  was accomplished under helium flow ( $100 \text{ cm}^3 \text{ min}^{-1}$ ) at 673 K for 4 h, with a heating rate of  $5 \text{ K min}^{-1}$ . Eight different catalysts were obtained. For comparative purposes, a composite of the oxidized activated carbon (ACox) and cerium oxide (sample  $\text{ACox-CeO}_2$ ) with a similar amount of  $\text{CeO}_2$  (21.5%) was prepared by precipitation, according to the procedure described by Orge et al. [7]

The textural properties of the prepared materials were determined by  $\text{N}_2$  and  $\text{CO}_2$  adsorption at 77 and 273 K, respectively, on a Coulter Omnisorp 610 system. Before measurements, the samples were dried at 383 K for 12 h and out-gassed at 523 K under vacuum. The micropore volume,  $V_0$  for  $\text{N}_2$  and  $V_{\text{CO}_2}$  for  $\text{CO}_2$  adsorption, was calculated by application of the Dubinin–Radushkevich (DR) equation. The volume of mesopores,  $V_{\text{meso}}$ , was estimated by subtracting the volume of micropores  $V_0$  from the total, estimated by the uptake at a relative pressure of 0.95. Specific surface area was calculated using the BET method in the relative pressure range 0.05–0.12.

The determination of the amount and types of surface oxygen complexes in the carbon supports was accomplished by temperature-programmed decomposition (TPD) under helium. Samples (between 150 and 200 mg) were placed in a U-shaped quartz cell and treated at 373 K for 1 h under a helium flow ( $50 \text{ cm}^3 \text{ min}^{-1}$ ). Then, the temperature was raised at  $10 \text{ K min}^{-1}$  up to 1250 K. The decomposition products (carbon monoxide, carbon dioxide and water) were monitored by on-line mass spectrometry.

The determination of the  $\text{pH}_{\text{PZC}}$  of the carbon supports was carried out as follows [18]: 20 mL of NaCl 0.01 M solution was placed in

a closed Erlenmeyer flask; the pH was adjusted to a value between 3 and 10 by adding HCl 0.1 M or NaOH 0.1 M; then, 0.050 g of each sample was added and the final pH measured after 24 h under stirring at room temperature. Blank experiments (without the carbon material) were carried out in order to subtract the variation of pH caused by the effect of  $\text{CO}_2$  present in head space. The  $\text{pH}_{\text{PZC}}$  is the point where the curve  $\text{pH}_{\text{final}}$  vs.  $\text{pH}_{\text{initial}}$  crosses the line  $\text{pH}_{\text{initial}} = \text{pH}_{\text{final}}$ .

Powder X-ray diffraction patterns were recorded on a JSO Deby-flex 2002 system, from Seifert, fitted with a Cu cathode and a Ni filter, using a  $20^\circ \text{C min}^{-1}$  scanning rate. The average crystal size for  $\text{CeO}_2$  was estimated by application of the Scherrer equation to the (1 1 1) ceria diffraction peak.

Selected samples were analyzed by X-ray photoelectron spectroscopy (XPS): Ce(III)/AC-w, Ce(IV)/AC-w, Ce(III)/ACox-k and Ce(III)/ACox-w. XPS was performed with a VG Scientific ESCALAB 200A spectrometer. XPS data corresponding to Ce 3d spectra were fitted using the software *XPSpeak*. To minimize the number of degrees of freedom of the curve fitting procedure, constraints on the binding energy (BE), full width at half maximum (FWHM) and peak areas were applied to each doublet pair.

Two samples were analyzed by scanning electron microscopy (SEM), Ce(III)/ACox-k and ACox-CeO<sub>2</sub>, in order to compare the morphologies of the ceria-activated carbon composite and the highly dispersed ceria catalyst. The semi-quantitative elemental analysis was also obtained by energy dispersive X-ray spectroscopy (EDS). SEM/EDS analyses were performed on a JEOL JSM 35C/Noran Voyager system.

### 2.2. Catalytic tests

The prepared catalysts were tested in the ozonation of oxalic acid (Fluka, 99%) and aniline (Sigma Aldrich, 99%). For comparative purposes, single ozonation experiments were also carried out. The ozonation experiments were carried out in a laboratory scale reactor (ca. 1 L) equipped with agitation and a circulation jacket. The agitation was done using a CAT R50D stirrer. The pollutant solution and the catalyst were introduced initially through an opening at the top of the reactor. The feeding of the gaseous flow was made through a porous plate placed at the bottom of the reactor. Ozone was produced from pure oxygen in a BMT 802X ozone generator. The concentration of ozone in the gas phase was monitored with a BMT 964 ozone analyser. Ozone in the gas phase leaving the reactor was removed in a series of gas-washing bottles filled with iodide potassium (KI) solution.

In each ozonation experiment the reactor was filled with 700 mL of organic solution (oxalic acid: 5 mM, or aniline: 1 mM) at the natural pH. In catalytic ozonation experiments, 100 mg of catalyst (particle size: 100–300  $\mu\text{m}$ ) was introduced in the reactor. These experimental conditions were more severe than those used in previous studies (oxalic acid: 1 mM, 300 mg of catalyst) [3,6,17] because otherwise, due to the high activity of the prepared catalysts, differences in their catalytic performances could not be clearly detected. The experiments were carried out at constant gas flow rate ( $150 \text{ cm}^3 \text{ min}^{-1}$ ) and constant inlet ozone concentration ( $50 \text{ g m}^{-3}$ ). The stirring rate was maintained at 300 rpm in order to keep the reactor content perfectly mixed, and the temperature was set to 298 K. Samples were taken regularly for quantification of dissolved ozone by the indigo method [19]. In the adsorption experiments, the ozone-containing stream was replaced by an oxygen stream. In the experiments carried out in the presence of *tert*-butanol, a concentration of 10 mM of this radical scavenger was used. In cyclic experiments, the same procedure was followed and, after each run, the solution was filtered and the catalyst dried in order to be used in another run; this procedure was repeated two times.

Liquid samples were collected using a syringe at selected times and centrifuged prior to analysis. The concentration of the pollutants was followed by HPLC using a Hitachi Elite LaChrom HPLC equipped with a diode array detector. The stationary phase was an *YMC Hydrosphere C18* (250 mm  $\times$  4.6 mm) working at room temperature. Oxalic acid and aniline were analyzed under isocratic elution with a mixture of water, acetonitrile and *o*-phosphoric acid at pH 2.0 using a flow rate of 1.0 mL min<sup>-1</sup>. The retention times for oxalic acid and aniline were 7.1 and 3.7 min, respectively. The wavelength of 210 nm was used for quantitative measurements of the compounds. Calibration curves with nine points (0.05–7 mM) for oxalic acid and six points (0.05–1 mM) for aniline were determined. Linear responses were obtained in these ranges. The  $r^2$  values of calibration lines were 0.99872 and 0.99870 for oxalic acid and aniline, respectively. Limit of quantification (LOQ)=0.42 mM, limit of detection (LOD)=0.088 mM for oxalic acid, and LOQ=0.087 mM, LOD=0.013 mM for aniline were obtained. The degree of mineralization of aniline was obtained by Total Organic Carbon (TOC) analysis in a Shimadzu TOC-5000A analyser.

### 3. Results and discussion

#### 3.1. Characterization of the materials

##### 3.1.1. Surface chemistry

The surface oxygen groups on both carbon supports, AC and AC<sub>ox</sub>, were characterized by temperature-programmed decomposition (TPD). It is well known that these surface functionalities decompose upon heating in an inert atmosphere, evolving CO and CO<sub>2</sub> at different temperatures [20,21]. Fig. 1 shows the evolution of CO (Fig. 1a) and CO<sub>2</sub> (Fig. 1b) for both supports. As it can be clearly seen, the parent carbon AC contains surface oxygen groups that decompose evolving mainly CO at high temperatures

**Table 1**

CO and CO<sub>2</sub> evolved from the supports in TPD experiments.

Sample	CO (mmol g <sup>-1</sup> )	CO <sub>2</sub> (mmol g <sup>-1</sup> )	CO/CO <sub>2</sub>	pH <sub>PZC</sub>
AC	0.257	0.043	6.0	7.8
AC <sub>ox</sub>	0.432	0.078	5.5	6.8

(maximum decomposition rate at 1050 K), whereas CO<sub>2</sub> evolution at lower temperatures is minimal. This CO evolution is related to the decomposition of phenol, ether and carbonyl/quinone surface groups [20,21]. The amounts of CO and CO<sub>2</sub> evolved from carbon AC<sub>ox</sub> are higher than those evolved from the parent carbon (AC), indicating the effect of the oxidation treatment. It can be seen in Fig. 1 that the TPD profile of sample AC<sub>ox</sub> shows a CO<sub>2</sub> evolution peak centered at 550 K, which corresponds to the decomposition of carboxylic surface groups. Other more stable functionalities, such as lactones, are responsible for CO<sub>2</sub> evolution at higher temperatures. AC<sub>ox</sub> presents a CO/CO<sub>2</sub> ratio lower than the original carbon, indicating that its basicity is lower. This observation is consistent with the pH<sub>PZC</sub> results present in Table 1. In conclusion, the oxidation treatment of the parent carbon AC yields a support (AC<sub>ox</sub>) with a more hydrophilic and acidic surface, due to the presence of surface oxygen functionalities. These characteristics are expected to affect the interactions with the ceria precursors.

##### 3.1.2. Textural properties

Fig. 2 shows the N<sub>2</sub> adsorption–desorption isotherms for both series, AC and AC<sub>ox</sub>, modified by CeO<sub>2</sub> deposition and after a decomposition treatment in helium (original activated carbons are also included). Textural properties obtained from these isotherms are summarized in Table 2. A mixed type I and IV isotherm is observed in all cases, with a large adsorption capacity at low relative pressures (adsorption in micropores), together with an hysteresis loop at high relative pressures, characteristic of activated carbons with a certain proportion of mesoporosity (Table 2). As it can be seen, the oxidation treatment led to a slight reduction in the BET surface area for the AC<sub>ox</sub> sample (from 1527 to 1422 m<sup>2</sup> g<sup>-1</sup>), with a corresponding reduction in the volume of micropores (Table 1, Table 2). In the case of samples supported on original AC, the deposition of CeO<sub>2</sub> produced a noticeable decrease in the surface area for those samples utilizing the Ce(III) precursor, which is accompanied with a significant reduction of the volume of micro and mesopores. Remarkably, the samples impregnated with the Ce(IV) precursor did not show a significant change in surface area. These results suggest that impregnation with the Ce(IV) precursor leads to optimum CeO<sub>2</sub> dispersion over the carbonaceous support, in close agreement with the CeO<sub>2</sub> particle size obtained by XRD (Table 1). While the methodologies involving the Ce(IV) precursor resulted in a high CeO<sub>2</sub> dispersion when using either water or acetone, in the case of using the Ce(III) precursor the dissolution with acetone led to lower dispersion compared with the same process using water. For the samples supported on AC<sub>ox</sub>, a decrease in the BET surface area and pore volumes was only observed when acetone was used as solvent. In these cases, a higher CeO<sub>2</sub> dispersion was obtained.

##### 3.1.3. XPS results

The oxidation state of the surface cerium species on selected cerium oxide/activated carbon samples was characterized by XPS. According to the literature [22], Ce 3d XPS spectra of Ce<sup>4+</sup> can be resolved into six features. If some Ce<sup>3+</sup> species are present, then two additional peaks and the corresponding satellites are necessary to describe spectra. Furthermore, Ce<sup>4+</sup> and Ce<sup>3+</sup> always show peaks at 882.5 and 916.5 eV as well as at 885.0 and 903.7 eV, which are considered fingerprints characterizing +4 and +3 oxidation states,

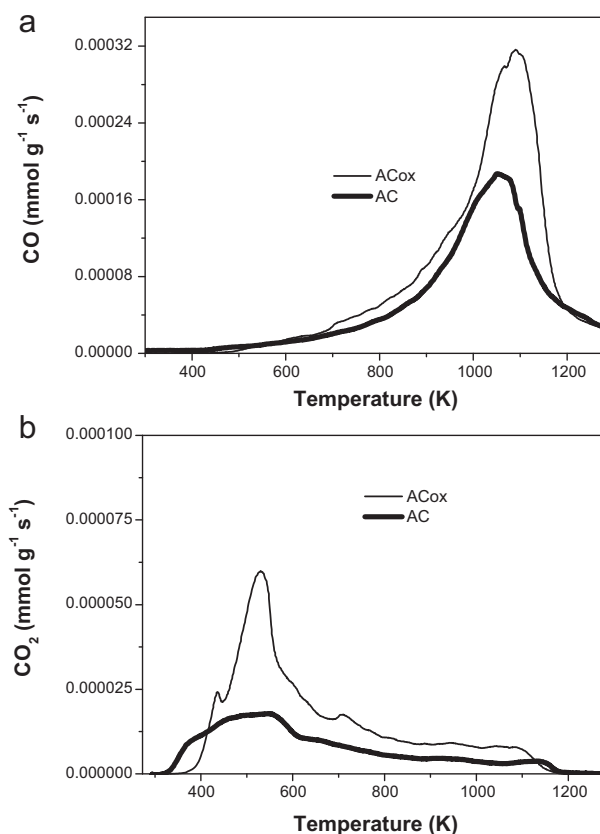


**Fig. 1.** TPD spectra of the carbon supports. (a) CO; (b) CO<sub>2</sub>.

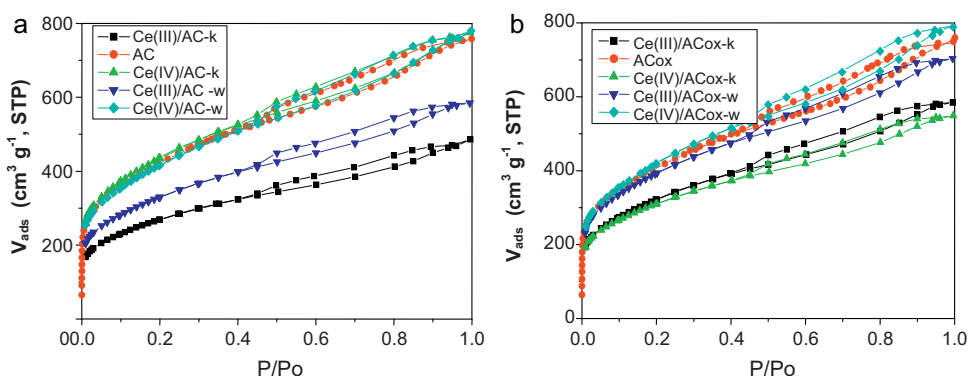


Fig. 2.  $N_2$  adsorption/desorption isotherms at 77 K for the catalysts prepared using (a) AC and (b)  $AC_{ox}$ , as support.

Table 2

Textural properties of the different catalysts, and  $CeO_2$  crystallite sizes obtained by XRD.

Sample	$S_{BET}$ ( $m^2 g^{-1}$ )	$V_0$ ( $cm^3 g^{-1}$ )	$V_{meso}$ ( $cm^3 g^{-1}$ )	$V_{CO_2}$ ( $cm^3 g^{-1}$ )	% Mesopores	Ceria crystallite size (nm)
AC	1527	0.52	0.64	0.32	55.2	–
Ce(III)/AC-k	968	0.36	0.36	0.20	50.0	5.2
Ce(III)/AC-w	1187	0.44	0.45	0.26	50.6	4.1
Ce(IV)/AC-k	1567	0.57	0.58	0.28	50.4	3.4
Ce(IV)/AC-w	1504	0.55	0.63	0.29	53.4	3.5
$AC_{ox}$	1422	0.50	0.66	0.34	56.9	–
Ce(III)/ $AC_{ox}$ -k	1164	0.43	0.48	n.d. <sup>a</sup>	52.7	4.5
Ce(III)/ $AC_{ox}$ -w	1405	0.51	0.68	n.d. <sup>a</sup>	57.1	6.5
Ce(IV)/ $AC_{ox}$ -k	1103	0.41	0.44	n.d. <sup>a</sup>	51.8	4.2
Ce(IV)/ $AC_{ox}$ -w	1515	0.55	0.65	n.d. <sup>a</sup>	54.2	5.7
$AC_{ox}-CeO_2$	1179	0.22	0.72	n.d. <sup>a</sup>	76.6	n.d. <sup>a</sup>

<sup>a</sup> n.d.: not determined.

respectively [23]. Although Ce 3d spectra of samples present the characteristic features of cerium (IV) oxide, the coexistence of both  $Ce^{3+}$  and  $Ce^{4+}$  species must be considered in order to obtain a good fitting of the experimental data. Spectra were fitted with ten peaks

[24,25], as it can be seen in Fig. 3. The experimental and fitted Ce 3d spectra of samples Ce(III)/ $AC_{ox}$ -k, Ce(III)/AC-w, Ce(IV)/AC-w and Ce(III)/ $AC_{ox}$ -w are shown in Fig. 3a, b, c and d, respectively. In the Ce  $3d_{5/2}$  spin-orbit split doublet for  $Ce^{4+}$ ,  $v_0$  and  $v_2$

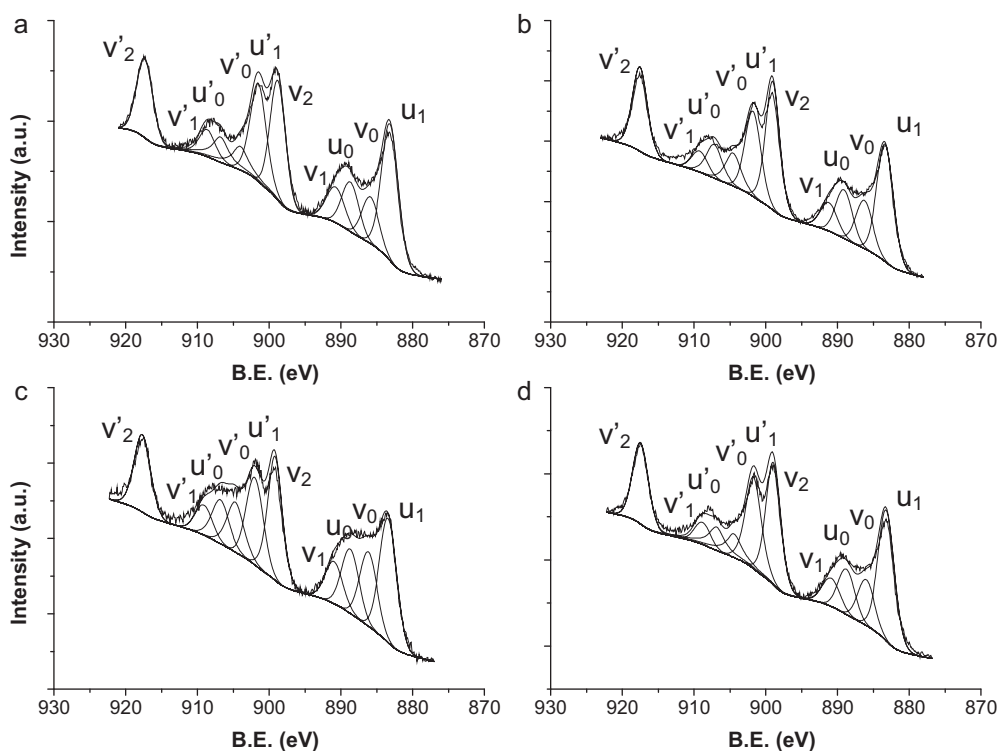


Fig. 3. Experimental and fitted Ce 3d XPS spectra of the samples (a) Ce(III)/ $AC_{ox}$ -k, (b) Ce(III)/AC-w, (c) Ce(IV)/AC-w and (d) Ce(III)/ $AC_{ox}$ -w.



**Table 3**

Relative percentage of  $\text{Ce}^{3+}$  and atomic percentage of the elements on the surface, measured by XPS.

Samples	$\text{Ce}^{3+}$ (%)	at. %		
		C	O	Ce
Ce(III)/AC <sub>ox</sub> -k	49.3	54.4	32.3	13.3
Ce(III)/AC-w	46.9	45.5	37.7	16.8
Ce(IV)/AC-w	45.6	65.7	26.1	8.2
Ce(III)/AC <sub>ox</sub> -w	48.5	48.9	36.4	14.7

components represent the intense peaks and  $\nu_1$  a weak satellite (see Fig. 3). Correspondingly,  $\nu_0'$  and  $\nu_2'$  components represent the Ce  $3d_{3/2}$  doublet intense peaks, and  $\nu_1'$  the associated weak satellite [25–29]. For the oxidation state +3, the main components  $u_0$  and  $u_1$  characterize Ce  $3d_{5/2}$ , and  $u_0'$  and  $u_1'$  the Ce  $3d_{3/2}$  contribution [25,30,31]. Two different approaches have been followed to evaluate the degree of ceria reduction from the XPS spectra. On one hand, some authors have used the relative area of the Ce  $3d_{3/2}$  peak at ca. 917 eV ( $\nu_2'$ ), characteristic of  $\text{CeO}_2$  (it is absent in pure  $\text{Ce}_2\text{O}_3$ ) to describe the total amount of cerium present as  $\text{Ce}^{4+}$  [32–34]. However, it has been shown that this procedure may lead to incorrect quantitative results [35]. The second approach takes into consideration the relative intensity of the  $u_0$ ,  $u_0'$ ,  $u_1$  and  $u_1'$  peaks, as representative of  $\text{Ce}^{3+}$ , in the total Ce 3d region [35–39]. The percentages of  $\text{Ce}^{3+}$  determined by this method are reported in Table 3.

The results obtained from the four samples analyzed by XPS (see Table 3) allow to shed some light on the effect of the support, precursor and solvent used in the preparation of the catalysts in the oxidation states of the surface cerium species. Comparing the effect of the cerium precursor using an aqueous solution (samples Ce(III)/AC-w and Ce(IV)/AC-w), it can be observed that the precursor “Ce(III)” leads to a slightly higher percentage of  $\text{Ce}^{3+}$  in the activated carbon surface than the precursor “Ce(IV)” (46.9% vs. 45.6%). Concerning the effect of the support, the oxidized activated carbon contributed to increase the relative percentage of  $\text{Ce}^{3+}$  in the surface of the carbon (48.5%) compared to the commercial (non-oxidized) activated carbon (46.9%). Regarding the effect of the solvent used to dissolve the precursor, a slight increase of  $\text{Ce}^{3+}$  is observed when acetone was used instead of water (49.3% vs. 48.5%). In summary, sample Ce(III)/AC<sub>ox</sub>-k has the highest percentage of  $\text{Ce}^{3+}$  on the surface (49.3%), whereas sample Ce(IV)/AC-w has the lowest (45.6%). Sample Ce(IV)/AC-w also presents the lowest atomic percentages of cerium and oxygen on the surface.

### 3.2. Catalytic tests

#### 3.2.1. Ozonation of oxalic acid

Oxalic acid has been identified as one of the most common final oxidation products from organic compounds degradation. This fact can be explained by the low reaction rate constants reported in the literature for the reaction between ozone and oxalic acid or the corresponding anions ( $k < 0.04 \text{ M}^{-1} \text{ s}^{-1}$  [40]); the compounds with low reactivity towards ozone may be oxidized by secondary oxidants such as hydroxyl radicals produced during the decomposition of ozone in aqueous solution. Actually, oxalic acid reacts with  $\text{HO}^\bullet$  radicals at a much higher rate ( $k \approx 10^6 \text{ M}^{-1} \text{ s}^{-1}$ ) [41]. Heterogeneous catalytic ozonation has been proven to be efficient in the removal of this kind of organic compounds. Several catalysts have been tested and it has been shown that they improve the mineralization of oxalic acid in aqueous solution [3,6,42–46]. In this work, the ozonation of this carboxylic acid in the presence of the prepared catalysts was investigated at natural pH (approximately 3). For comparative purposes, experimental results obtained with the two parent activated carbon samples and by single ozonation were included. The results obtained are depicted in Fig. 4. Some experiments were carried out in duplicate and the maximum relative deviation obtained was 2%. The analytical measurements were also performed in duplicate with a maximum relative error of  $\pm 0.5\%$ .

It was observed that single ozonation only removed about 55% of the oxalic acid in solution after 5 h, while the addition of the prepared catalysts significantly enhanced its mineralization. All ceria/activated carbon samples act efficiently as ozonation catalysts, even better than the corresponding parent activated carbons. In fact, the simultaneous use of ozone and ceria/activated carbon samples resulted in the removal of more than 85% of oxalic acid after 3 h, compared to less than 60% with the activated carbons.

Comparing the performance of both activated carbons, the activated carbon without treatment (AC) was more efficient to remove the oxalic acid in solution than the oxidized activated carbon (AC<sub>ox</sub>). This observation was expected because the surface chemistry of activated carbons influences their performance as catalyst for this type of reactions [2,47]. This is related to a low content of surface oxygenated groups with electron withdrawing properties, and to the existence of delocalized  $\pi$  electrons in the basal planes, which are characteristics of basic activated carbons [48], resulting in a higher electron density on the surface when compared with acidic activated carbons. Thus, basic activated carbons favor the adsorption step of ozone molecules as a result of the dispersive interactions with those electrons. On the other hand, they act as an electron source favoring the reduction of ozone molecules, which

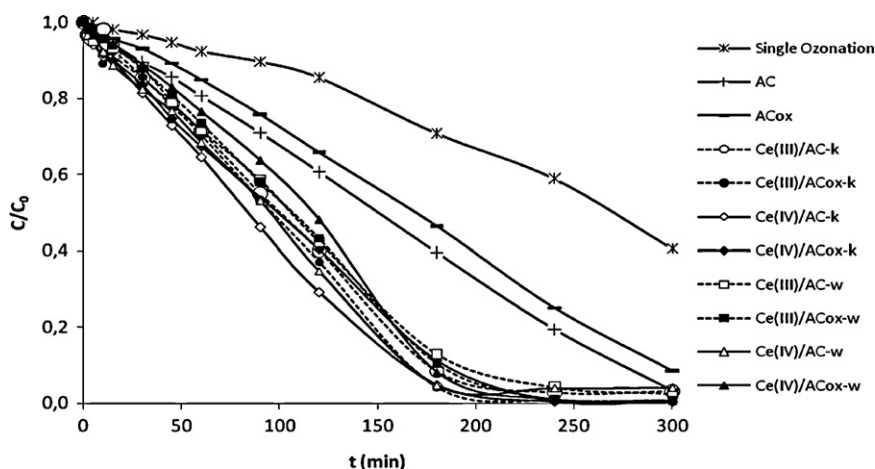
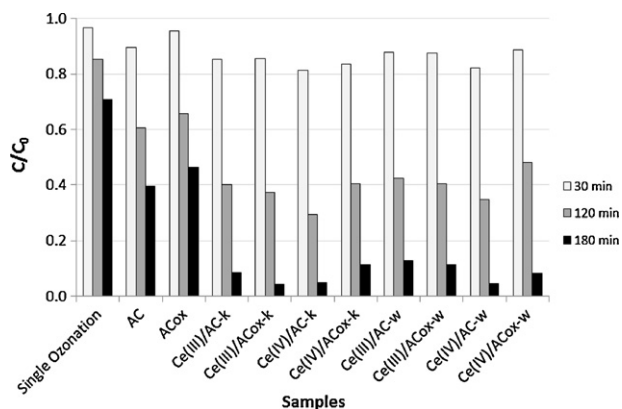


Fig. 4. Evolution of the dimensionless concentration of oxalic acid at natural pH ( $\sim 3$ ) during catalytic and non-catalytic ozonation ( $C_0 = 5 \text{ mM}$ , catalysts =  $0.14 \text{ g L}^{-1}$ ).



**Fig. 5.** Dimensionless concentration of oxalic acid at natural pH (~3) during catalytic and non-catalytic ozonation (times selected: 30, 120 and 180 min).

have the ability to withdraw electrons from a given source (electrophilic behavior) [49]. The results obtained from TPD (Table 1) show that the oxidized sample ( $AC_{ox}$ ) presents an amount of surface oxygenated acidic groups (mainly released as  $CO_2$ ) about twice as much as the commercial sample (AC), which justifies a better catalytic performance of AC in the oxalic acid ozonation, when compared with  $AC_{ox}$ .

The ozonation of oxalic acid in the presence of ceria/activated carbon samples showed excellent results, leading to nearly complete mineralization of oxalic acid after 3–4 h. Actually, these materials are more effective to remove oxalic acid when compared to the parent activated carbons. In addition, the textural parameters (see Table 2) generally show that these ceria/activated carbon samples present lower specific surface areas than the parent activated carbons, where oxalic acid and molecular ozone can adsorb and react. Thus, the presence of cerium oxide in the prepared catalysts enhances the catalytic performance of the activated carbons. This fact can be explained by the availability of free electrons on the surface of the activated carbon that may contribute to the formation of  $Ce^{3+}$  species, which are effective in the decomposition of ozone into  $HO^\bullet$  radicals, as it was proved in previous studies [1,6].

The effect of the support, precursor and solvent used for the preparation of ceria/activated carbon samples on their performance for the ozonation of oxalic acid was evaluated at three reaction times (30, 120 and 180 min). Fig. 5 shows that the removal of oxalic acid is very similar after 30 min for all tests, but for longer times the differences among samples are evident. To evaluate the influence of the support, the remaining parameters were fixed (precursor and solvent). Independently of the solvent used in the catalyst preparation, when “Ce(IV)” is used as precursor, the support that leads to the highest removals of oxalic acid is AC, whereas using “Ce(III)” the best support is  $AC_{ox}$ . Concerning the precursor, the materials prepared from “Ce(IV)” present best removals when the support is AC, regardless of the solvent, whereas in the presence of  $AC_{ox}$  as support, “Ce(III)” is generally the precursor that leads to the best results. Comparing the solvents, the ceria/activated carbon samples prepared with acetone are, in general, more active catalysts for ozonation than the same materials prepared using water as solvent.

The ceria/activated carbon samples prepared from “Ce(IV)” using acetone or water as solvent (Ce(IV)/AC-k and Ce(IV)/AC-w, respectively) lead to the highest mineralization of oxalic acid. These materials present the highest specific surface areas ( $1567$  and  $1504\text{ m}^2\text{ g}^{-1}$ , respectively) where both oxalic acid and ozone can adsorb and react, as well as the highest micropore volume. They also present the smallest  $CeO_2$  crystal size (3.4 and 3.5 nm, respectively). Consequently, these samples have the highest metal oxide surface area, favoring the ozone decomposition into hydroxyl

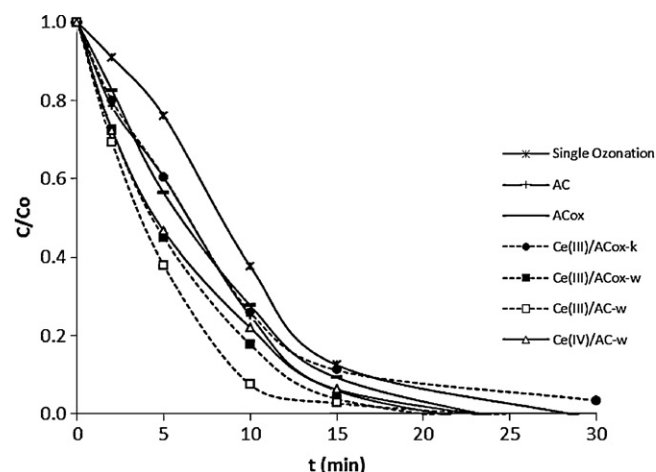


**Fig. 6.** Evolution of the dimensionless concentration of aniline at natural pH (~6.4) during catalytic and non-catalytic ozonation ( $C_0 = 1\text{ mM}$ , catalysts  $= 0.14\text{ g L}^{-1}$ ).

radicals. Nevertheless, sample Ce(III)/ $AC_{ox}$ -k also has an excellent catalytic performance in the removal of oxalic acid, despite it does not present neither a high specific surface area ( $1164\text{ m}^2\text{ g}^{-1}$ ) nor a small diameter of metal oxide particles (4.5 nm), when compared with the other two samples mentioned. Moreover,  $AC_{ox}$  has a large amount of oxygen containing surface groups with the ability of attracting  $\pi$  electrons. However, the excellent results obtained in the presence of Ce(III)/ $AC_{ox}$ -k can be explained by the XPS results. In fact, this sample presents the highest relative percentage of  $Ce^{3+}$  on the surface, which is effective in the decomposition of ozone into  $OH^\bullet$  radicals. The remaining samples have similar performances in the removal of oxalic acid.

Cyclic experiments using Ce(III)/ $AC_{ox}$ -k were carried out with the purpose of assessing the eventual deactivation during mineralization of oxalic acid. It was verified that there is only a slight decrease of activity from the first to the second cycle, remaining stable thereafter.

### 3.2.2. Ozonation of aniline

The ozonation of aniline was carried out at the natural solution pH (approximately 6.4). The ozonation kinetic experiments were performed in the presence of the four samples that were characterized by XPS: Ce(III)/AC-w, Ce(IV)/AC-w, Ce(III)/ $AC_{ox}$ -k, Ce(III)/ $AC_{ox}$ -w. In addition to the catalytic ozonation in the presence of these prepared catalysts, experiments in the presence of the two parent activated carbon samples were also carried out for comparison. Both aniline and TOC decay were followed during 300 min, and the corresponding experimental data are presented in Fig. 6 and Fig. 7, respectively.

Fig. 6 shows that ozonation by itself enables a fast decay of the aniline concentration and, under the selected experimental conditions, the elimination of this compound from aqueous solution is achieved in less than 30 min. This is because ozone selectively attacks activated aromatic rings present in compounds, which is the case of aniline. In fact, the amino group ( $-NH_2$ ) present in the aniline molecule is electron donating, activating the aromatic ring by increasing its electron density. Furthermore, aromatic compounds such as aniline, have a high delocalization of electrons and exhibit improved reactivity towards ozone. The simultaneous use of ozone and activated carbon (either AC or  $AC_{ox}$ ) resulted in a slight increase in the removal rate of aniline comparing with single ozonation, which might be explained by a sum of contributions of direct and indirect ozonation, and adsorption on activated carbon. Comparing the parent activated carbons with the corresponding ceria/activated carbon samples, no important differences

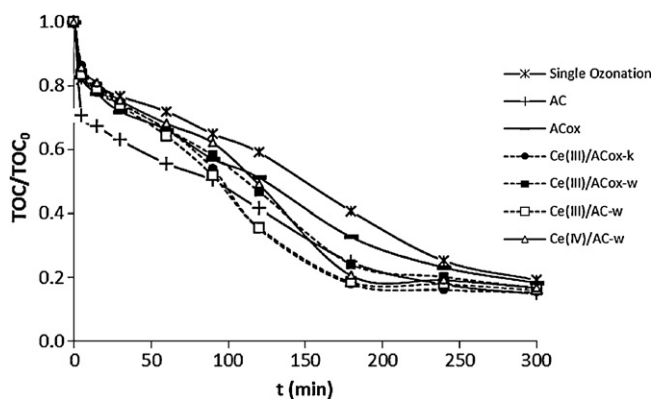


Fig. 7. Evolution of the dimensionless TOC concentration during catalytic and non-catalytic ozonation of aniline at natural pH ( $\sim 6.4$ ) ( $C_0 = 1$  mM, catalysts =  $0.14$  g L $^{-1}$ ).

were observed in the aniline removal. On the other hand, if TOC results are analyzed, the catalytic performances are relatively different, as it can be seen in Fig. 7. The activated carbon without treatment (AC) has an enhanced effect in the aniline mineralization, particularly in the first minutes, owing to the strong contribution of adsorption on the activated carbon surface. At pH around 6.4, aniline is present in solution in its molecular form. It adsorbs on the activated carbon by interaction between the free electrons of the activated carbon surface and the electrons of the aromatic ring [50]. Since AC has a higher electron density, it adsorbs more aniline than sample AC<sub>ox</sub>. Thus, aniline adsorption on the activated carbon contributes for its partial removal from solution. Nevertheless, the best TOC results are obtained in the presence of ceria/activated carbon samples, except for short reaction times. This catalytic effect results from a cooperative action between activated carbon and cerium oxide. The former is thought to be able to promote the reduction of Ce $^{4+}$  to Ce $^{3+}$  species, due the existence of delocalized  $\pi$  electrons on the basal planes of the activated carbon, enhancing its catalytic properties for the generation of HO $^{\bullet}$  radicals in solution [6]. Ce(III)/AC-w and Ce(III)/AC<sub>ox</sub>-k are the most active samples in aniline ozonation (see Fig. 8), since they surpass the performance of activated carbons after 90 min of reaction, whereas the remaining ceria/activated carbon catalysts need longer times (between 120 and 180 min). The most efficient catalysts in the mineralization of aniline do not present neither the highest surface areas nor the highest micropore volumes. Moreover, the average diameter of metal oxide particles dispersed on the surface of these catalysts is not the smallest. However, according to the XPS results, the highest relative percentage of Ce $^{3+}$  on the surface of the material is obtained

for the Ce(III)/AC<sub>ox</sub>-k sample, which shows the best results in the mineralization of aniline. Therefore, these observations indicate that the relative percentage of Ce $^{3+}$  in the surface of the catalysts plays a leading role in the ozonation of aniline. Ce(III)/AC-w also presents a similar performance compared to the previous sample, indicating that the support is also important, since it may play two different roles. On one hand, using oxidized activated carbon (AC<sub>ox</sub>) as support, the relative percentage of Ce $^{3+}$  species in the surface of the material increases (see Table 3), which is effective in the decomposition of ozone into HO $^{\bullet}$  radicals [6]; on the other hand, AC<sub>ox</sub> has a lower electron density than AC, and its contribution to the aniline removal by adsorption is lower. The remaining two samples, Ce(III)/AC<sub>ox</sub>-w and Ce(IV)/AC-w, present lower performances in the aniline mineralization, as it can be seen in Fig. 8. Ce(III)/AC<sub>ox</sub>-w contains a high relative percentage of Ce(III) on the surface. However, the average diameter of the metal oxide particles dispersed on its surface is the largest (6.5 nm), which may disfavor its performance as ozonation catalyst, since the metal oxide surface area, where ozone is decomposed into hydroxyl radical, is smaller. Concerning Ce(IV)/AC-w, this catalyst presents similar results as the previous sample, despite containing the smallest relative percentage of Ce $^{3+}$  on the surface. This observation may suggest that the textural properties and the particle diameter of ceria crystallites also have some influence in the catalytic results, since Ce(IV)/AC-w presents a high specific surface area ( $1504$  m $^2$  g $^{-1}$ ) where aniline, their intermediates and ozone can adsorb and react, as well as a high micropore volume and a low diameter of the metal oxide particles (3.5 nm).

Despite the different performances of the catalysts along the reaction time, they tend towards similar mineralization values for high reaction times (remaining TOC between 15 and 20%). This is probably due to formation of by-products that are very refractory to ozonation. A previous study showed that oxalic and oxamic acids are the major final oxidation by-products from catalytic ozonation of aniline [51], which suggests that the remaining TOC observed in the final solutions may be mainly originated by the presence of oxamic acid since these catalysts are effective for the oxalic acid removal.

### 3.2.3. Considerations on the reaction mechanism and the role of catalysts preparation

The ozonation of organic compounds involves a number of complex reactions and many mechanistic approaches have been presented in the literature. In heterogeneous catalytic ozonation both surface and liquid bulk reactions can occur, involving molecular ozone, HO $^{\bullet}$  radicals and surface oxygenated radical species. Activated carbon catalyzes the decomposition of ozone in the aqueous phase by the formation of surface oxygenated radical species as well as promoting the formation of HO $^{\bullet}$  radicals in solution [39]. In the case of the ozonation catalyzed by metal oxides, the proposed mechanisms generally assume that the adsorption of organic molecules and ozone takes place on the surface of the catalyst [52]. The interaction of ozone with the metal oxide surface results in the formation of free radicals that can initiate a radical chain type reaction both on the surface of the catalyst and in the liquid phase, leading to the production of HO $^{\bullet}$  radicals [1,44]. For cerium oxide catalysts, it has been shown that the free radical oxidation mainly occurs in the solution [6]. Samples AC and Ce(III)/AC<sub>ox</sub>-k were selected for additional experiments in the presence of *tert*-butanol, a well known HO $^{\bullet}$  radical scavenger, in order to investigate the mechanism of the oxalic acid and aniline ozonation in the presence of ceria/activated carbon catalysts. The results obtained for oxalic acid removal (see Fig. 9) show that ozonation in the presence of activated carbon was not significantly affected by the presence of the radical scavenger during the first 30 min. This observation indicates that the catalytic ozonation of the oxalic acid occurs mainly on the surface of the activated carbon, but hydroxyl radical species

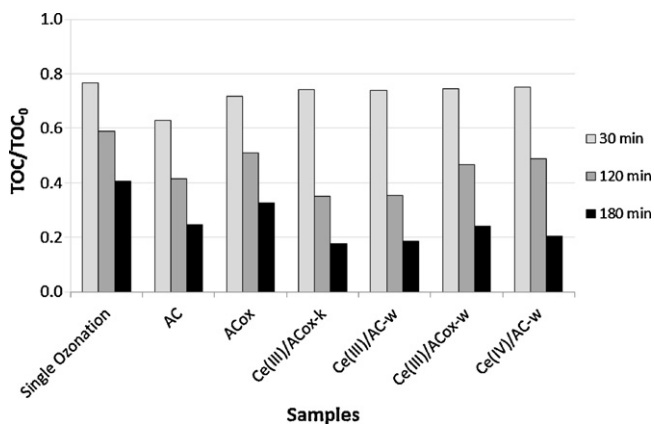
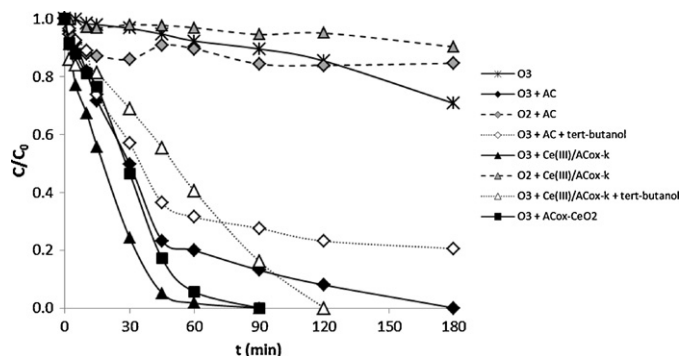


Fig. 8. Dimensionless TOC concentration during catalytic and non-catalytic ozonation of aniline at natural pH ( $\sim 6.4$ ) (times selected: 30, 120 and 180 min).



**Fig. 9.** Evolution of the dimensionless concentration of oxalic acid at natural pH ( $\sim 3$ ) during adsorption, catalytic ozonation and effect of *tert*-butanol ( $C_0$ , oxalic acid = 1 mM,  $C_0$ , *tert*-butanol = 10 mM, catalysts =  $0.14 \text{ g L}^{-1}$ ).

in solution also contributes to the oxalic acid removal, especially for long reaction times where the solution pH increases (pH is approximately 5 after 180 min). The ozonation catalyzed by Ce(III)/AC<sub>ox</sub>-k is more severely affected by the presence of *tert*-butanol, the double reaction time being necessary to completely remove oxalic acid. Thus, it can be concluded that oxalic acid is oxidized not only on the surface of the ceria/activated carbon catalyst, which is mainly due to the contribution of activated carbon, but also in solution involving hydroxyl radical species. Concerning the results of aniline removal, Fig. 10 shows that ozonation of aniline in the presence of both AC and Ce(III)/AC<sub>ox</sub>-k is not inhibited by the presence of *tert*-butanol and that adsorption is only responsible for about 15% of the aniline removal. These results demonstrate that aniline molecule is easily oxidized directly by ozone, due to the presence of the strong activating group  $-\text{NH}_2$ , which activates the aromatic ring by increasing the electron density by a resonance donating effect, as discussed before. Nevertheless, as mentioned above, the main advantage of using a catalyst in the ozonation of aniline is in its mineralization. However, due to the important contribution of *tert*-butanol to the TOC value of the solution, it was not possible to follow this parameter.

The results obtained in this study show a strong catalytic effect in the materials prepared, characterized by the presence of cerium oxide highly dispersed in activated carbon for the mineralization of both oxalic acid and aniline. In these ceria/activated carbon catalysts, the carbon material is supposed to play different roles. On one hand, it provides a high specific surface area where both organic compounds and ozone can adsorb and react. On the other hand, the availability of free electrons on the surface of the carbon material may contribute to the formation of  $\text{Ce}^{3+}$  species, which are effective in the decomposition of ozone into  $\text{HO}^\bullet$  radicals. Therefore, it is

assumed that the reaction mechanism responsible for the efficiency of the catalysts prepared in the present work comprises both surface reactions and reactions in the liquid bulk. However, depending on the studied compound, the catalytic effect of the ceria/activated carbon samples is different.

In general, for oxalic acid ozonation, the catalysts prepared from the precursor “Ce(IV)” dispersed on AC samples (Ce(IV)/AC-k and Ce(IV)/AC-w) lead to the highest mineralization, owing to the presence of the highest specific surface areas and micropore volumes, as well as the smallest diameter of metal oxide particles. On the contrary, the aniline mineralization is favored by the presence of catalysts prepared from the precursor “Ce(III)” dispersed on AC samples (Ce(III)/AC<sub>ox</sub>-k and Ce(III)/AC-w), since the relative percentage of  $\text{Ce}^{3+}$  in the surface of the catalysts seems to play the leading role in the process. In summary, it can be concluded that the use of AC as support favors the removal of both organic compounds studied, and the precursor to use in the catalysts preparation depends on the target pollutant, i.e. the “Ce(III)” precursor favors the mineralization of aniline, while oxalic acid removal is favored by the “Ce(IV)” precursor.

The catalyst Ce(III)/AC<sub>ox</sub>-k stands out among the prepared catalysts for the mineralization of both oxalic acid and aniline. This sample presents the highest relative percentage of Ce(III) in the surface, which emphasizes the idea that the decomposition of ozone into  $\text{HO}^\bullet$  radicals by Ce(III) species on the surface of the catalysts is essential for their efficiency in the ozonation of the organic compounds studied.

Finally, the performance of the Ce(III)/AC<sub>ox</sub>-k catalyst was compared with a ceria/carbon composite with a similar composition (sample AC<sub>ox</sub>-CeO<sub>2</sub>) for the oxidation of oxalic acid; the corresponding results are depicted in Fig. 9. Details about the preparation of this type of composites can be found elsewhere [7]. A better performance for the highly dispersed ceria catalyst was observed, which may be mainly justified by its largest metal oxide surface area, evidenced in the micrographs obtained by SEM analysis of both catalysts. Fig. 11 shows SEM micrographs of ceria highly dispersed on carbon or in a composite form, where the differences in the particle diameter are clear. In the ceria/activated carbon composite (AC<sub>ox</sub>-CeO<sub>2</sub>) it is possible to identify carbon enriched areas (dark areas, Z2) and Ce enriched zones (clear areas, Z1). In the catalyst Ce(III)/AC<sub>ox</sub>-k clear and dark areas are not observed, which indicates that the followed method allows to obtain a much better dispersion of ceria on activated carbon than in the ceria/activated carbon composite, leading to a better performance of this material as ozonation catalyst.

The dissolved ozone concentration during ozonation experiments can support the mechanism proposed in this work. In the case of oxalic acid, which is refractory to ozone, the dissolved ozone

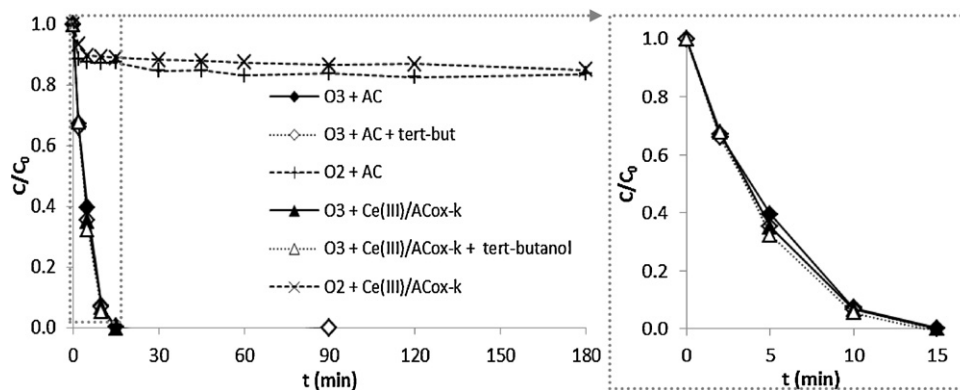


**Fig. 10.** Evolution of the dimensionless concentration of aniline at natural pH ( $\sim 6.4$ ) during adsorption, catalytic ozonation and effect of *tert*-butanol ( $C_0$ , aniline = 1 mM,  $C_0$ , *tert*-butanol = 10 mM, catalysts =  $0.14 \text{ g L}^{-1}$ ).



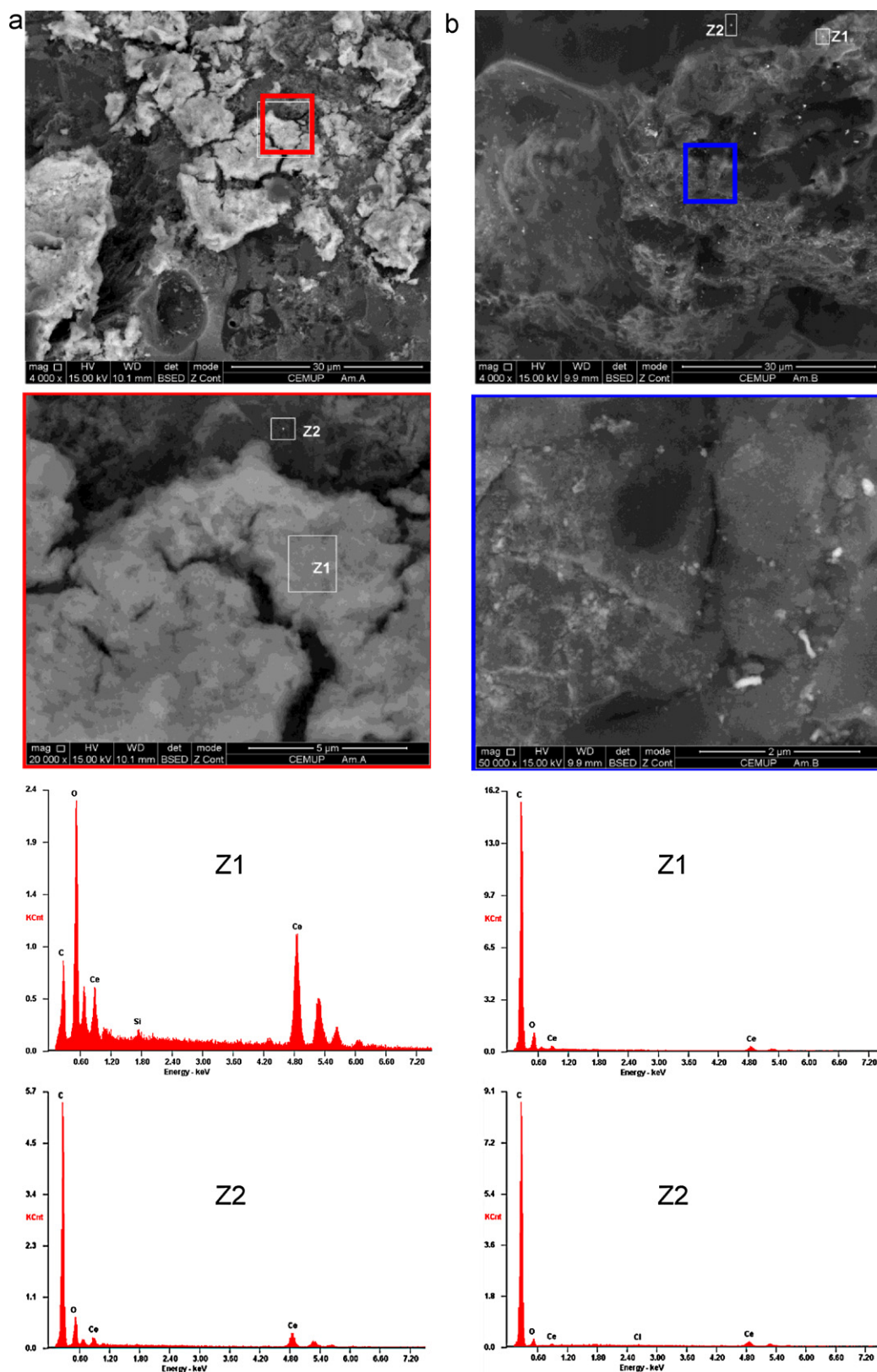


Fig. 11. SEM micrographs and EDS analyses of samples (a)  $\text{AC}_{\text{ox}}\text{-CeO}_2$  and (b)  $\text{Ce(III)/AC}_{\text{ox-k}}$ .

concentration obtained during single ozonation ( $7.5 \text{ mgO}_3 \text{ L}^{-1}$ , at the end of reaction) was higher than in presence of activated carbon ( $5.0 \text{ mgO}_3 \text{ L}^{-1}$ , at same time). This is due to the role of the activated carbon surface in the oxidation of oxalic acid, which involves not only  $\text{HO}^\bullet$  radicals, but also surface oxygenated radicals

resultant from the reaction between ozone and activated carbon. When ceria/activated carbon samples are used, the dissolved ozone concentration is even smaller ( $1.4 \text{ mgO}_3 \text{ L}^{-1}$ , at the end of reaction), which indicates that cerium present on the surface of activated carbon is effective in the decomposition of ozone into  $\text{HO}^\bullet$

radicals. In the case of aniline, for an early stage of the reaction, the concentration of dissolved ozone in solution is very small, independently of the presence or absence of the catalyst, because ozone is mainly consumed in the degradation of the aromatic moieties and unsaturated compounds. As the refractory character of the solution increases, the trend of the dissolved ozone concentration becomes similar to that of the oxalic acid degradation.

#### 4. Conclusions

Several catalysts of cerium oxide highly dispersed on activated carbon were prepared, characterized and afterwards investigated as ozonation catalysts in the mineralization of two organic compounds (oxalic acid and aniline). For comparative purposes, ozonation results obtained in the absence of catalyst and in the presence of the parent activated carbon samples were also performed.

The prepared catalysts have better performances than the parent activated carbons in the ozonation of the selected organic compounds, showing a clear synergic effect between activated carbon and cerium oxide.

The use of AC as support favors the removal of both organic compounds. In general, catalysts prepared from the “Ce(III)” precursor favors the mineralization of aniline, while oxalic acid removal is favored by catalysts prepared from the “Ce(IV)” precursor.

The efficiency of the catalysts in the ozonation of the studied organic compound is mainly affected by the amount of Ce<sup>3+</sup> species on the surface, since they are active for the decomposition of ozone into HO• radicals. However, in the oxalic acid ozonation, the specific surface area and the particle diameter of ceria crystallites also play an important role, while for aniline these parameters are not so relevant.

The mechanism of the ozonation catalyzed by ceria/activated carbon catalysts is believed to comprise both surface reactions, similar to what occurs with activated carbon promoted ozonation, and also reactions in the liquid bulk involving HO• radicals, resultant not only from the catalytic decomposition of ozone on the surface of the activated carbon but mainly from the presence of cerium oxide. It is assumed that the existence of delocalized electrons on the basal planes of carbon materials contributes to the formation of Ce<sup>3+</sup> species, which are active for the decomposition of ozone into HO• radicals.

These highly dispersed ceria on activated carbon catalysts present better performance than a ceria/carbon composite with a similar composition, which may be mainly justified by its largest metal oxide surface area.

#### Acknowledgments

This work was carried out with the support of Acção Integrada Luso-Espanhola 31/08 - HP2007-0106 and project PEst-C/EQB/LA0020/2011, financed by FEDER through COMPETE - Programa Operacional Factores de Competitividade and by FCT - Fundação para a Ciência e a Tecnologia. Financial support from Generalitat Valenciana (PROMETEO/2009/002 - FEDER) is also gratefully acknowledged. A.G.G. acknowledges the Grant received from FCT (BD/45826/2008). The authors are indebted to Dr. Carlos M. Sá (CEMUP) for assistance with SEM and XPS analyses.

#### References

- [1] B. Legube, N. Karpel Vel Leitner, *Catalysis Today* 53 (1999) 61–72.
- [2] P.C.C. Faria, J.J.M. Órfão, M.F.R. Pereira, *Water Research* 39 (2005) 1461–1470.
- [3] P.C.C. Faria, J.J.M. Órfão, M.F.R. Pereira, *Applied Catalysis B: Environmental* 79 (2008) 237–243.
- [4] F.J. Beltrán, J.F. García-Araya, I. Giraldez, *Applied Catalysis B: Environmental* 63 (2006) 249–259.
- [5] M. Sánchez-Polo, U. von Gunten, J. Rivera-Utrilla, *Water Research* 39 (2005) 3189–3198.
- [6] P.C.C. Faria, J.J.M. Órfão, M.F.R. Pereira, *Catalysis Communications* 9 (2008) 2121–2126.
- [7] C.A. Orge, J.J.M. Órfão, M.F.R. Pereira, *Applied Catalysis B: Environmental* 102 (2011) 539–546.
- [8] J.C. Serrano-Ruiz, E.V. Ramos-Fernández, J. Silvestre-Albero, A. Sepúlveda-Escribano, F. Rodríguez-Reinoso, *Materials Research Bulletin* 43 (2008) 1850–1857.
- [9] D. Zhang, L. Shi, H. Fu, J. Fang, *Carbon* 44 (2006) 2853–2855.
- [10] E. Ramos-Fernández, J. Serrano-Ruiz, J. Silvestre-Albero, A. Sepúlveda-Escribano, F. Rodríguez-Reinoso, *Journal of Materials Science* 43 (2008) 1525–1531.
- [11] D. Zhang, T. Yan, L. Shi, C. Pan, J. Zhang, *Applied Surface Science* 255 (2009) 5789–5794.
- [12] D. Zhang, H. Mai, L. Huang, L. Shi, *Applied Surface Science* 256 (2010) 6795–6800.
- [13] D. Zhang, C. Pan, J. Zhang, L. Shi, *Materials Letters* 62 (2008) 3821–3823.
- [14] P.C.C. Faria, J.J.M. Órfão, M.F.R. Pereira, *Applied Catalysis B: Environmental* 83 (2008) 150–159.
- [15] K. Pachhade, S. Sandhya, K. Swaminathan, *Journal of Hazardous Materials* 167 (2009) 313–318.
- [16] N.M. Mahmoodi, *Desalination* 279 (2011) 332–337.
- [17] P.C.C. Faria, J.J.M. Órfão, M.F.R. Pereira, *Chemosphere* 67 (2007) 809–815.
- [18] J. Rivera-Utrilla, I. #M. Bautista-Toledo, A. Ferro-García, C. Moreno-Castilla, *Journal of Chemical Technology & Biotechnology* 76 (2001) 1209–1215.
- [19] H. Bader, J. Hoigné, *Water Research* 15 (1981) 449–456.
- [20] J.L. Figueiredo, M.F.R. Pereira, M.M.A. Freitas, J.J.M. Órfão, *Carbon* 37 (1999) 1379–1389.
- [21] J.L. Figueiredo, M.F.R. Pereira, M.M.A. Freitas, J.J.M. Órfão, *Industrial Engineering Chemistry Research* 46 (2007) 4110–4115.
- [22] M. Nolan, J.E. Fearon, G.W. Watson, *Solid State Ionics* 177 (2006) 3069–3074.
- [23] H.-X. Mai, L.-D. Sun, Y.-W. Zhang, R. Si, W. Feng, H.-P. Zhang, H.-C. Liu, C.-H. Yan, *The Journal of Physical Chemistry B* 109 (2005) 24380–24385.
- [24] B.M. Reddy, G. Thirumurthulu, L. Katta, Y. Yamada, S.-E. Park, *The Journal of Physical Chemistry C* 113 (2009) 15882–15890.
- [25] Tana, M. Zhang, J. Li, H. Li, Y. Li, W. Shen, *Catalysis Today* 148 (2010) 179–183.
- [26] W. Shan, X. Dong, N. Ma, S. Yao, Z. Feng, *Catalysis Letters* 131 (2009) 350–355.
- [27] K. Niesz, D.E. Morse, *Nano Today* 5 (2010) 99–105.
- [28] R.K. Hailstone, A.G. DiFrancesco, J.G. Leong, T.D. Allston, K.J. Reed, *The Journal of Physical Chemistry C* 113 (2009) 15155–15159.
- [29] X.H. Lu, X. Huang, S.L. Xie, D.Z. Zheng, Z.Q. Liu, C.L. Liang, Y.X. Tong, *Langmuir* 26 (2010) 7569–7573.
- [30] K. Zhou, Z. Yang, S. Yang, *Chemistry of Materials* 19 (2007) 1215–1217.
- [31] C. Sun, J. Sun, G. Xiao, H. Zhang, X. Qiu, H. Li, L. Chen, *Journal of Physical Chemistry B* 110 (2006) 13445–13452.
- [32] F.B. Noronha, E.C. Fendley, R.R. Soares, W.E. Alvarez, D.E. Resasco, *Chemical Engineering Journal* 82 (2001) 21–31.
- [33] J.Z. Shyu, K. Otto, W.L.H. Watkins, G.W. Graham, R.K. Belitz, H.S. Gandhi, *Journal of Catalysis* 114 (1988) 23–33.
- [34] J.Z. Shyu, W.H. Weber, H.S. Gandhi, *Journal of Physical Chemistry* 92 (1988) 4964–4970.
- [35] J. Silvestre-Albero, F. Rodríguez-Reinoso, A. Sepúlveda-Escribano, *Journal of Catalysis* 210 (2002) 127–136.
- [36] A. Laachir, V. Perrichon, A. Badri, J. Lamotte, E. Catherine, J.C. Lavalley, J. El Fallah, L. Hilaire, F. Le Normand, E. Quémère, G.N. Sauvion, O. Touret, *Journal of the Chemical Society Faraday Transactions* 87 (1991) 1601–1609.
- [37] B. Ernst, L. Hilaire, A. Kiennemann, *Catalysis Today* 50 (1999) 413–427.
- [38] M.S.P. Francisco, V.R. Mastelaro, P.A.P. Nascente, A.O. Florentino, *Journal of Physical Chemistry B* 105 (2001) 10515–10522.
- [39] C.A. Orge, J.J.M. Órfão, M.F.R. Pereira, A.M. Duarte de Farias, R.C.R. Neto, M.A. Fraga, *Applied Catalysis B: Environmental* 103 (2011) 190–199.
- [40] J. Hoigné, H. Bader, *Water Research* 17 (1983) 173–183.
- [41] K. Sehested, N. Getoff, F. Schwoerer, V.M. Markovic, S.O. Nielsen, *The Journal of Physical Chemistry* 75 (1971) 749–755.
- [42] R. Andrezzi, A. Insola, V. Caprio, R. Marotta, V. Tufano, *Applied Catalysis A: General* 138 (1996) 75–81.
- [43] F.J. Beltrán, F.J. Rivas, R. Montero-de-Espinosa, *Applied Catalysis B: Environmental* 47 (2004) 101–109.
- [44] C. Cooper, R. Burch, *Water Research* 33 (1999) 3695–3700.
- [45] C.A. Orge, J.P.S. Sousa, F. Gonçalves, C. Freire, J.J.M. Órfão, M.F.R. Pereira, *Catalysis Letters* 132 (2009) 1–9.
- [46] A.G. Gonçalves, J.L. Figueiredo, J.J.M. Órfão, M.F.R. Pereira, *Carbon* 48 (2010) 4369–4381.
- [47] J. Rivera-Utrilla, M. Sánchez-Polo, *Applied Catalysis B: Environmental* 39 (2002) 319–329.
- [48] C.A. Leon y Leon, J.M. Solar, V. Calemme, L.R. Radovic, *Carbon* 30 (1992) 797–811.
- [49] P.C.C. Faria, J.J.M. Órfão, M.F.R. Pereira, *Industrial & Engineering Chemistry Research* 45 (2006) 2715–2721.
- [50] P.C.C. Faria, J.J.M. Órfão, J.L. Figueiredo, M.F.R. Pereira, *Applied Surface Science* 254 (2008) 3497–3503.
- [51] P.C.C. Faria, J.J.M. Órfão, M.F.R. Pereira, *Catalysis Letters* 127 (2009) 195–203.
- [52] F.P. Logemann, J.H.J. Annee, *Water Science and Technology* 35 (1997) 353–360.